Spin-wave Spectroscopy on Ferromagnetic Thin Film Using Vector Network Analyzer

Dr. Haiming Yu and Prof. Dirk Grundler

Physik-Department E10 Raum 2313

email:haiming.yu@ph.tum.de

(Dated: February 21, 2013)

I. INTRODUCTION

A. Spin wave and Magnonics

Magnonics is a research field in nanoscience whose purpose is to explore spin waves, i.e. magnons, to store, carry and process information. Magnons are elementary spin excitations in magnetic materials which exhibit a wave-like state. These can either be localized or propagate through the solid.

One of the key points of the field is that the wavelength of magnons is orders of magnitude shorter than that of electromagnetic waves (photons) of the same frequency.This means that magnonics fosters the development of nanoscale devices and enables nano-optics with spin waves as well as high-density integration.

B. All electrical spin-wave spectroscopy

To explore collective spin excitations in nanostructured ferromagnets we make use of an all-electrical approach. Using optimized coplanar waveguides (CPWs) and a vector network analyzer (VNA) we have set up a broadband spin wave spectrometer. It covers the frequency range from some 10 MHz up to 26 GHz. The CPW provides, both, the microwave field excitation of the nanomagnets' spins and the detection of spin waves. The detected voltage is induced by the precessing spins. The magnets are either monolithically integrated to the CPW or mounted in a flip-chip configuration. The CPW containing the nanomagnets is located between the electromagnet poles, which can provide magnetic field up to 1.8T. By this means, we control the magnetic history and the magnetic configuration. If the inner conductor of the CPW is tapered down to the 1 m scale the sensitivity increases such that the spin excitation of a single Permalloy micromagnet can be studied. The broad frequency range allows us to study spin-wave excitations (i) in a wide range of magnetic fields, (ii) in different materials, (iii) for different magnetic configurations of one and the same sample and (iv) to follow the magnetic field dispersion of excitations. The latter enables us to classify spin-wave excitations and to understand in detail the microscopic origin.

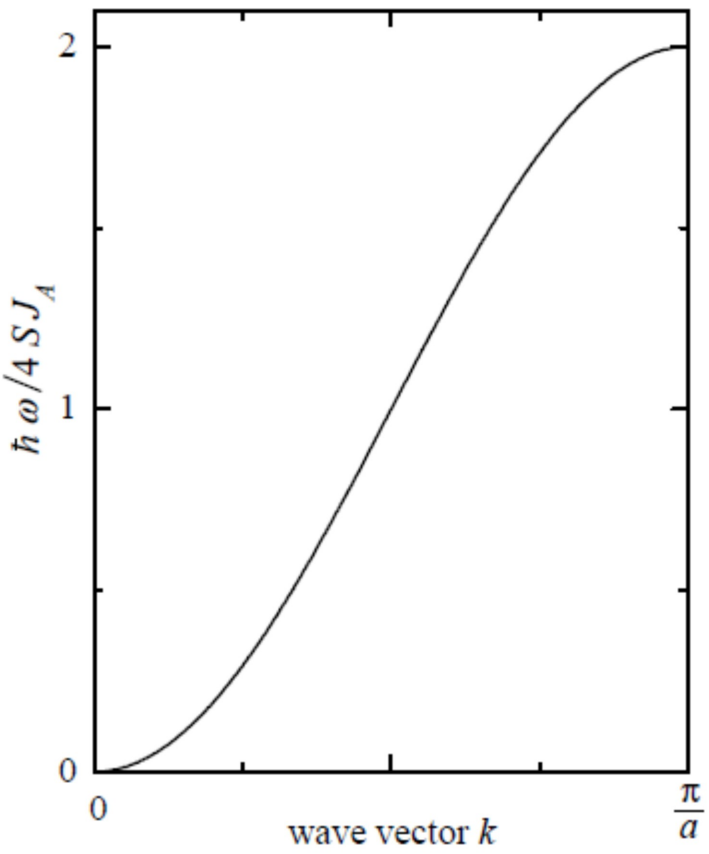

FIG. 1. Wavevector dispersion $\omega(k)$ of a spin wave in a ferromagnet exhibiting a homogeneous internal field, i.e., the magnet is saturated and geometrical boundaries do not play a role. The frequency is given in units of S (spin) and J_{A} (exchange integral). For clarity a one-dimensional ferromagnet is assumed.

C. Spin wave on ferromagnetic materials

In this lab exercise, we study spin wave on a ferromagnetic thin film where (i) the magnetization M is saturated due to a large external field H and (ii) the static internal field H_{int} is homogeneous. In this case a low-energy collective spin excitation can exhibit a wave vector $k = 0$ where all spins precess coherently around H. This excitation is called uniform spin precession and might be detected by an FMR experiment. In case of a BLS experiment, one is able to transfer momentum to the spin system. Thereby the excitation of spin waves with $k \neq 0$ becomes possible. Such excitations, called magnons, propagate within the magnetic film and exhibit a characteristic dispersion $\omega(\vec{k})$. A typical dispersion curve that

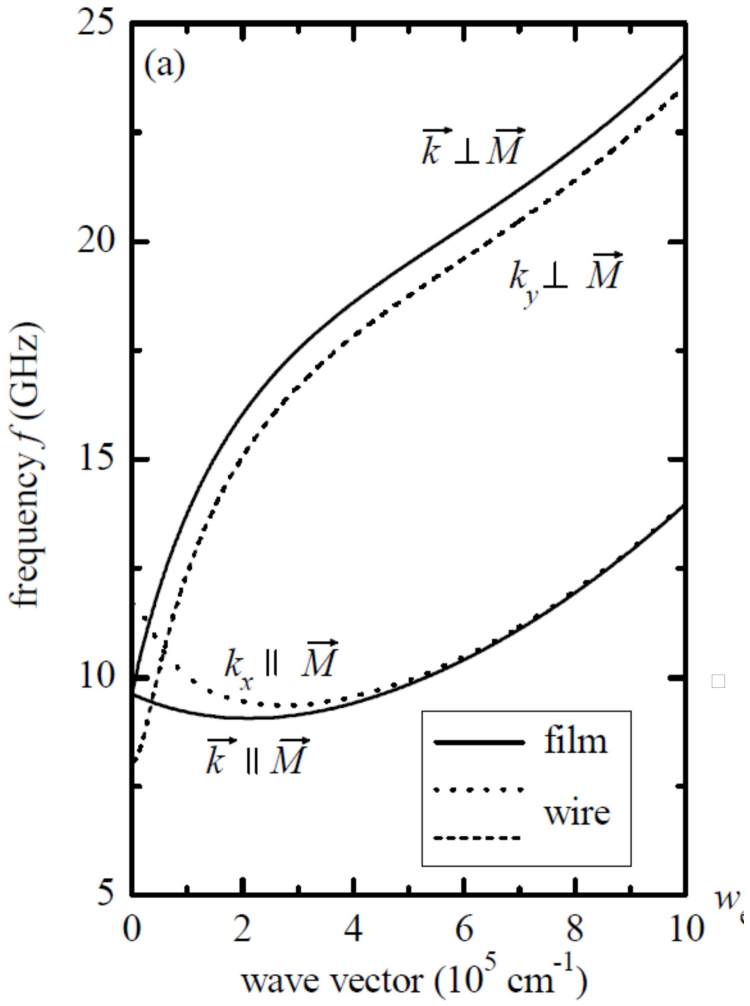

FIG. 2. (a) Wavevector dispersions at $\mu_0 H = 100$ mT for an infinite film for two orientations: $\vec{k} \parallel \vec{M}$ (bottom solid trace) and $\vec{k} \perp \vec{M}$ (upper solid trace). The dashed (dotted) trace reflects a wire with $w = 700$ nm which is magnetized transversely (longitudinally).

is often displayed in solid state textbooks is shown in Fig. 1. For clarity, we assume a one-dimensional ferromagnet with nearest-neighbor spin-spin interaction. The eigenfrequency of the spin wave increases monotonously with increasing wave vector k. Here it is important that only exchange contributions are considered. Approaching the Brillouin zone boundary at $k = \frac{2\pi}{\lambda} = \frac{\pi}{a}$, where a is the lattice constant, the wavelength λ becomes so short that neighboring spins are misaligned. Exchange interaction dominates the high eigenfrequency. For spin waves in microstructures it is important to consider also contributions which arise from both static and dynamic demagnetization fields, i.e., from dipolar interaction. In this

scenario the eigenfrequencies do not depend only on the absolute value of the wave vector $|\vec{k}|$ but also on the angle α enclosed by $\vec{k}$ and the magnetization $\vec{M}$. The solid lines in Fig. 2(a) are calculated and include both dipolar and exchange interactions. The depicted dispersion curves are valid for a sample where the magnetization $\vec{M}$ lies in the plane of the film and is collinear with the external magnetic field $\vec{H}$ [cf. Fig. 2(b)]. Spin waves with $\vec{k} = (k_x, k_y, k_z)$ propagate without restrictions only in the x, y plane. The top and bottom film surfaces impose a boundary condition on the wave vector k_z. In z direction a standing spin wave is formed and k_z becomes discrete according to $k_z = \frac{p\pi}{t}$. Here, t is the film thickness and $p = 0, 1, 2, ...$ We will discuss the lowest mode with $p = 0$ only. Considering unpinned spins at the surfaces the eigenmode is uniform in z direction. For the in-plane directions we now assume $k^2 = k_x^2 + k_y^2$. We distinguish two configurations in Fig. 2(a) depending on the angle α between $\vec{k}$ and $\vec{M}$. The angle turns out to be key for the spin wave dispersions $f\,(k) = \frac{\omega(k)}{2\pi}$: in case of $\alpha = \frac{\pi}{2}$, i.e. $\vec{k} \perp \vec{M}$, the eigenfrequency f is rising monotonously with k. These spin waves are called Damon-Eshbach modes (DE modes). In contrast, when $\alpha = 0$, i.e. $\vec{k} \parallel \vec{M}$, f shows a negative slope with k for small wave vectors. This is a so-called backward volume magnetostatic wave (BVMSW). The term "backward" originates from the negative group velocity $v_{\mathrm{gr}} = \frac{\partial\omega}{\partial k}$. The characteristics of both types of spin waves at small wave vector k (i.e. for long wavelengths) are dominated by the dipolar interactions which are of long range. This wavevector regime is thus termed "dipolar regime" in the literature. Here the contribution of the exchange energy is proportional to Jk^2 (J is the exchange constant and can, in principle, be calculated from the exchange integral J_{A} used in Fig. 1). Thus only for large values of k the exchange interaction takes over and leads to a quadratic increase of the corresponding eigenfrequencies. For high values of k both types of spin waves are therefore termed to be "exchange dominated". The two different dispersion curves displayed as solid traces in Fig. 2(a) reflect the upper and lower band edges of the spin wave band. Dispersion curves at angles $0 < \alpha < \frac{\pi}{2}$ fall between these band edges. Close to the Brillouin zone boundary the dispersions approach the characteristics of Fig. 1.

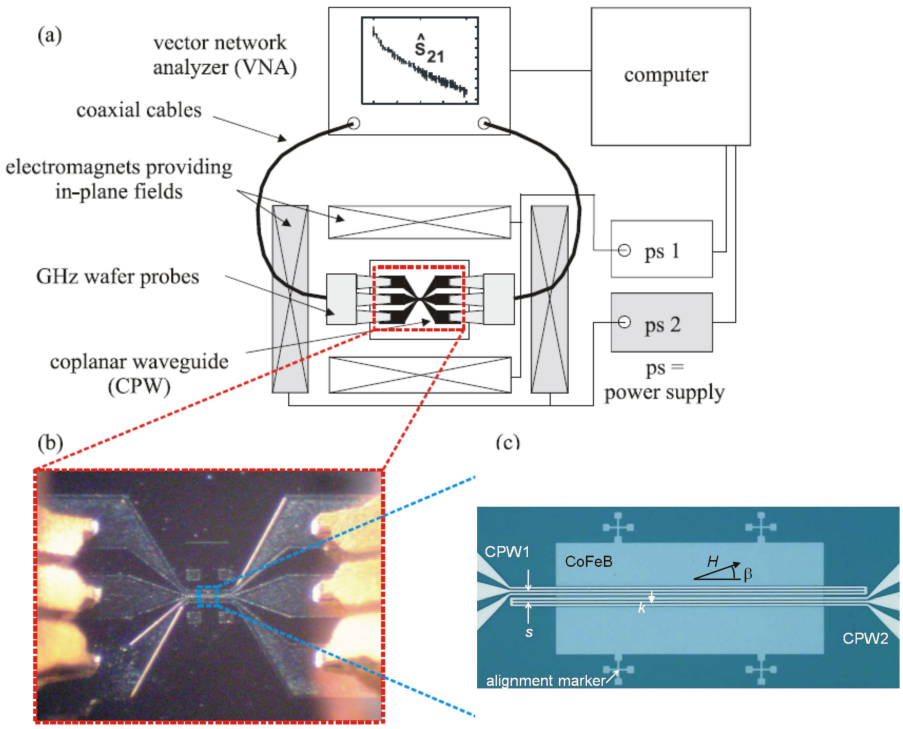

FIG. 3. (a) Block diagram of the broadband GHz spectrometer using a vector network analyzer. The VNA measures the complex scattering parameters (transmission: $\hat{S}_{21}$; reflection: $\hat{S}_{11}$) of a coplanar waveguide containing patterned ferromagnets. The CPW resides within two electromagnets generating an in-plane vector field. (b) GHz probes (yellow color) connect the CPW (light gray) which is tapered to a width of a few microns in its center. (c) Microscopy image of a CoFeB mesa with two integrated coplanar waveguides (CPWs). The center-to-center separation s of the two CPWs is 12 μm. Orientations of in-plane magnetic field H and wave vector k are sketched.

II. EXPERIMENTAL TECHNIQUES

A. Broadband spectroscopy

For the excitation and detection of magnetization dynamics of individual micro- and nanostructures or arrays of them we use a broadband GHz spectrometer operating at room temperature. It is depicted in Figs. 3(a) and (b). The CPW is optimized to exhibit low losses and a microwave impedance of $Z_0 = 50$ Ohm. This ensures high field amplitude $h_{\rm rf}$ at the sample's location and the efficient detection of the inductive response. Magnets are

integrated either directly on the GaAs substrate or on the central conductor of the CPW [Fig. 3(c)]. In both cases the magnetic devices are defined by electron beam lithography and lift-off processing. The CPW is fabricated from a metallic sandwich which consists of Cr, Ag and Au. Typically it is 160 nm thick. The gold serves as a caplayer to prevent the silver from oxidization. The thickness is chosen such that the Ohmic losses of the waveguide are small. The rms roughness of the CPW typically varies between 2.5 and 5 nm as measured by AFM. We use commercial microwave probes attached to micropositioners to connect the CPW to the VNA. The pitch of probes and contact pads is 250 μm. A microscope is needed to find the optimum position for the probes and thus minimize reflections [Fig. 3(b)]. Two orthogonal electromagnets, each with a maximum field of 100 mT, generate a field $\vec{H}$ in the plane of the magnetic sample. This field is used to define the magnetic history. To ensure optimum mechanical stability, the whole setup is mounted on an optical table with an active vibration damping system. It is remotely controlled by a personal computer.

In the following, we discuss details of the broadband spin wave spectroscopy using the VNA. In the experiment a sinusoidal high frequency current $i_{\rm rf}$ is passed through the CPW and produces the rf magnetic field $\vec{h}_{\rm rf}$. If $\vec{h}_{\rm rf}$ exerts a torque $\tau = \vec{h}_{\rm rf} \times \vec{M}$ on the magnetization $\vec{M} = \vec{M}_0 + \vec{m}(\omega, t)$ this gives rise to a time dependent magnetization $\vec{m}(\omega, t)$ that is orthogonal to $\vec{M}_0$. In the following, we will label the static magnetization by $\vec{M}_0$ and the dynamic component by $\vec{m}(\omega, t)$. Note that in our devices both quantities depend on the spatial coordinates, since we deal with inhomogeneous magnetization configurations, an inhomogeneous internal field and, as we will see, a finite wavevector $\vec{k}$ of the spin excitations. These aspects are all different if compared to the early work on FMR.

It is instructive to review the spatial profile of the excitation field. In the CPW we expect quasi-TEM modes to be present. As a consequence the field component in the propagation direction is negligible: $h_x \ll (h_y, h_z)$. Let us first assume a uniform current density over the CPW's central conductor with width w_C. The VNA-current induced field then lies almost perfectly in the plane of the magnets and perpendicular to the direction of the waveguide. In this case we obtain the magnetic field from $h_{\rm rf} = i_{\rm rf}/2w_C$. However, at GHz frequencies the current density is expected to be inhomogeneous and exhibit extremal values at the edges due to the self-inductance of the metallic conductors. Using free commercial software we model the current distribution at 20 GHz and determine the profile of $\vec{h}_{\rm rf}$ according to Biot and Savart's law . The in-plane component h_y is found to be almost constant over

the central conductor where the magnets are placed. We do not expect the enhancement of the in-plane field at the edges to play an important role as long as we choose the excitation field strength such that the linear regime of spin dynamics is addressed. The out-of-plane component h_z shows a high absolute value at the edges only outside the periodic arrays of nanomagnets. We therefore disregard this inhomogeneity when analyzing the experimental data. To substantiate this assumption we have performed simulations considering both the homogeneous and realistic excitation field profile. We have not obtained a difference in the calculated spin-wave absorption spectra.

The dynamics stimulated by $\vec{h}_{\mathrm{rf}}$

$$\vec{m}(\omega, t) = \hat{\chi}(\omega)\vec{h}_{\mathrm{rf}}(\omega, t)$$

induce a voltage V_{ind} in the waveguide. In the case of inhomogeneous magnetization patterns or rf excitation fields $\vec{m}$ depends also on the spatial coordinate $\vec{r}$ and on the wavevector $\vec{k}$. V_{ind} is calculated from reciprocity according to

$$V_{\mathrm{ind}} = \frac{\mu_0 N}{2} \int_{\mathrm{magnet}} \vec{h}_{\mathrm{rf}} \cdot \frac{\mathrm{d}\vec{m}(\vec{r}, t)}{\mathrm{d}t} \, \mathrm{d}\vec{r}. \tag{1}$$

Here, N is the number of magnets on the CPW and $\hat{\chi}$ the tensor of the complex magnetic susceptibility. The integration is performed over one of the magnets. Note that V_{ind} might be measured in reflection or in transmission geometry. Equation 1 shows that due to the distinct rf field profile present in a CPW only the transverse component of the dynamic magnetization, $\vec{m}_t = (m_y, m_z)$, is excited and detected. If magnets exhibit a small aspect ratio "thickness/width" m_y exceeds m_z by the inverse scaling factor, so the detection signal is dominated by m_y. When the dynamic magnetization is at resonance the phase shift between the exciting rf current i_{rf} and the induced current $i_{\mathrm{ind}} = Z_0^{-1} V_{\mathrm{ind}}$ is π. As a consequence absorption peaks occur at resonant spin wave eigenmodes of the magnets.

To extract the small inductive signal given by Eq. 1 from the complex electrodynamic response of the CPW including microwave probes and coaxial cables two experimental methods are applied: on the one hand we perform a thorough calibration of the whole setup and on the other hand we apply a difference detection scheme. The calibration is a two-step process. First a reference sample containing lithographically well-defined thin-film microwave devices like a through, an open and a matched load is used to calibrate the setup according to the so called through-reflection-match (TRM) method. From this calibration we obtain

parameters that remodel the dynamic response of the cables and connectors including the microwave probes. Second we replace the reference substrate by the CPW containing the nanomagnets and follow the TRM calibration a second time in such a manner that we consider the CPW as a through. In particular we apply a large in-plane magnetic field $\vec{H}$ perpendicular to the CPW's central conductor. In this case $\vec{M}$ and $\vec{h}_{\mathrm{rf}}$ are set to be parallel. This prevents us from exciting spin wave dynamics and V_{ind} is at minimum (see discussion below). After refining the characteristic TRM parameter set by this means the measurement technique is optimized to a degree that spin wave absorption features are seen directly on the display of the VNA. In our case the signal is about 10^{-3} to 10^{-2} dB.

We use a difference detection scheme to further improve the signal-to-noise and standing wave ratio. Prior to taking data under resonant conditions we acquire a reference spectrum with $\vec{M}_0$ being collinear with $\vec{h}_{\mathrm{rf}}$ to a very large extent. In this case, excitation and detection of magnetization dynamics are vanishingly small because (i) the torque on the static magnetization is tiny, i.e., $\tau = \vec{h}_{\mathrm{rf}} \times \vec{M}_0 \approx 0$, and (ii) the dynamic magnetization, if present, is oriented such that the induced voltage V_{ind} is very small. These arguments hold also for the second step of the TRM calibration scheme. Unsaturated edge regions in the magnets might exhibit $\vec{M}_0 \parallel$ CPW$\perp \vec{h}_{\mathrm{rf}}$, however the fraction of spins in such regions is assumed to be small. The voltage induced by an out-of-plane precessional component m_z is expected to be tiny also. One finds $\vec{h}_{\mathrm{rf}} \cdot \mathrm{d}\vec{m}/\mathrm{d}t \approx i\omega h_z\, m_z \approx 0$. This holds because $\vec{h}_{\mathrm{rf}}$ is mainly in plane of the CPW and $h_z \approx 0$ at the position of the magnets. As a consequence saturation in a direction perpendicular to the CPW provides a reference spectrum where absorption features due to spin waves are at minimum or even absent. This reference spectrum is then subtracted from the dynamic response measured in the desired magnetization configuration $\vec{M}$. The difference detection scheme is advantageous also because in long-term measurements we have observed that the electrical parameters drift and that the calibration degrades. Variations in the ambient conditions (room temperature, humidity) or magnetic field driven displacements of probes and cables might be responsible for the observed drifts.

B. Ferromagnetic thin film sample

The alloy CoFeB is used in magnetic tunnel junctions (MTJs), which form the basis for magnetic random access memory (MRAM), read heads in hard disk drives, as well as

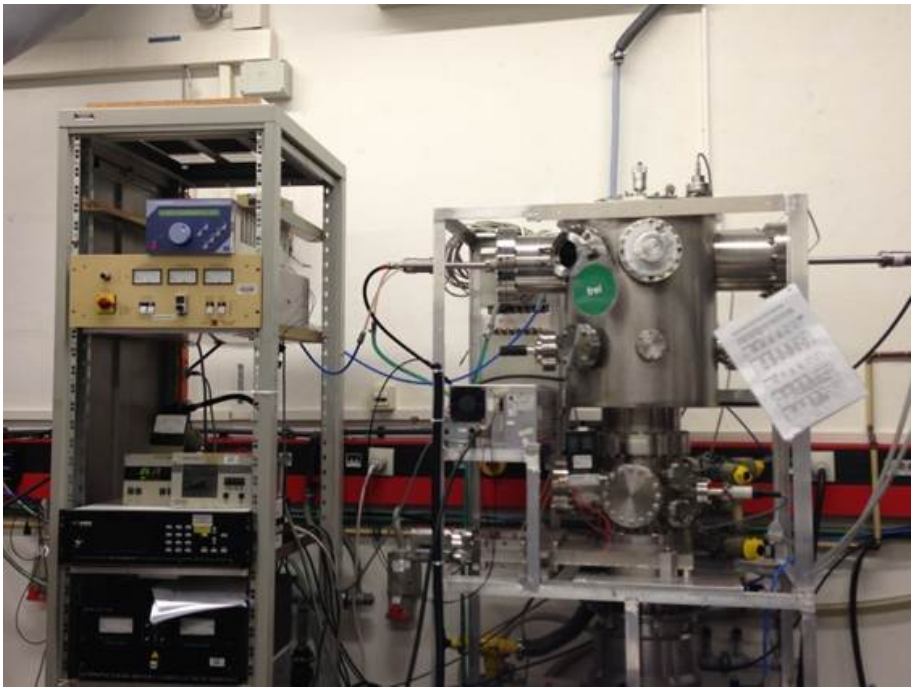

FIG. 4. Magnetron sputtering setup in E10 for $Co_{20}Fe_{60}B_{20}$ thin film deposition with Argon atmosphere.

spin-logic based devices. Thin films were prepared on semi-insulating GaAs substrates by magnetron sputtering in Argon atmosphere using a $Co_{20}Fe_{60}B_{20}$ target. Here we report data obtained on a 60 nm thick film forming a mesa with an area of 300 μm $\times$ 120 μm. A 5 nm thick layer of Al_2O_3 was grown by atomic layer deposition onto the mesa to ensure an electrical isolation for two open-ended metallic coplanar waveguides (CPWs) integrated by optical lithography. These two CPWs were designed to act as a spin wave emitter (CPW1) and detector (CPW2). The six conducting lines were 2 μm wide. The edge-to-edge separation between signal and ground lines was 1.6 μm. The distance s between the two inner conductors was 12 μm. To measure spin-wave propagation and extract the Gilbert damping parameter α_{i}, we connected a vector network analyzer to the CPWs. We measured transmission and reflection signals, respectively. The Fourier analysis of the microwave field generated around the inner conductor of CPW1 provided us with an excitation spectrum which contained two peaks I and II at wave vectors k_{I} and k_{II}, respectively. The wave vectors were perpendicular to the CPW. The magnetic field H was applied, both, in the film plane and in the out-of-plane direction.

III. PREVIEW QUESTIONS

1. What is a ferromagnet?
2. What is a spin wave? what is magnon?
3. What is a dispersion relation? What is the dispersion relation of spin waves?
4. What is a coplanar wave guide?
5. What equation is widely used to describe spin dynamics in ferromagnet?

IV. CONTROL AND SAFETY INSTRUCTION

A. Vector Network Analyzer (VNA)

Protection against electrostatic discharge (ESD) is essential while removing assemblies from or connecting cables to the network analyzer. Static electricity can build up on your body and can easily damage sensitive internal circuit elements when discharged. Static discharges too small to be felt can cause permanent damage. To prevent damage to the instrument: a. always have a grounded, conductive table mat in front of your test equipment.
b. always wear a grounded wrist strap, connected to a grounded conductive table mat, having a 1 $M\Omega$ resistor in series with it, when handling components and assemblies or when making connections.
c. always wear a heel strap when working in an area with a conductive floor. If you are uncertain about the conductivity of your floor, wear a heel strap.
d. always ground yourself before you clean, inspect, or make a connection to a static-sensitive device or test port. You can, for example, grasp the grounded outer shell of the test port or cable connector briefly.
e. always ground the center conductor of a test cable before making a connection to the analyzer test port or other static-sensitive device. This can be done as follows:
1. Connect a short (from your calibration kit) to one end of the cable to short the center conductor to the outer conductor.
2. While wearing a grounded wrist strap, grasp the outer shell of the cable connector.
3. Connect the other end of the cable to the test port and remove the short from the cable.
For our experiment, we have built a remote control system to automatically operate the

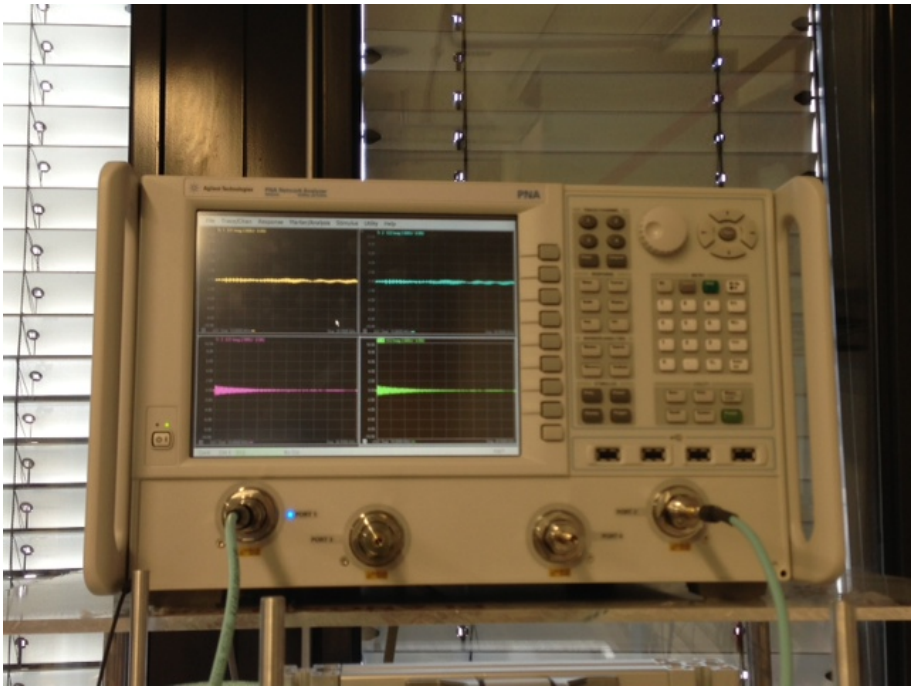

FIG. 5. Vector Network Analyzer

VNA, so without advisor's permission, please do not control from the front panel.

B. Power supply and electromagnet

The power supplies in your system may produce high voltages and energy hazards, which can cause bodily harm. Unless you are instructed otherwise, only trained service technicians are authorized to remove the covers and access any of the components inside the system. Since we can generate a fairly large magnetic field with the electromagnet, please do not come close to the magnet during operation!

V. LAB EXERCISE PROCEDURE AND MEASUREMENTS

A. Pre-measurement

1. turn on the power switch (on the wall), and make sure the cooling water is running.
2. turn the power supply to "stand-by" mode, turn the main switch on. (green button)
3. turn on the VNA .

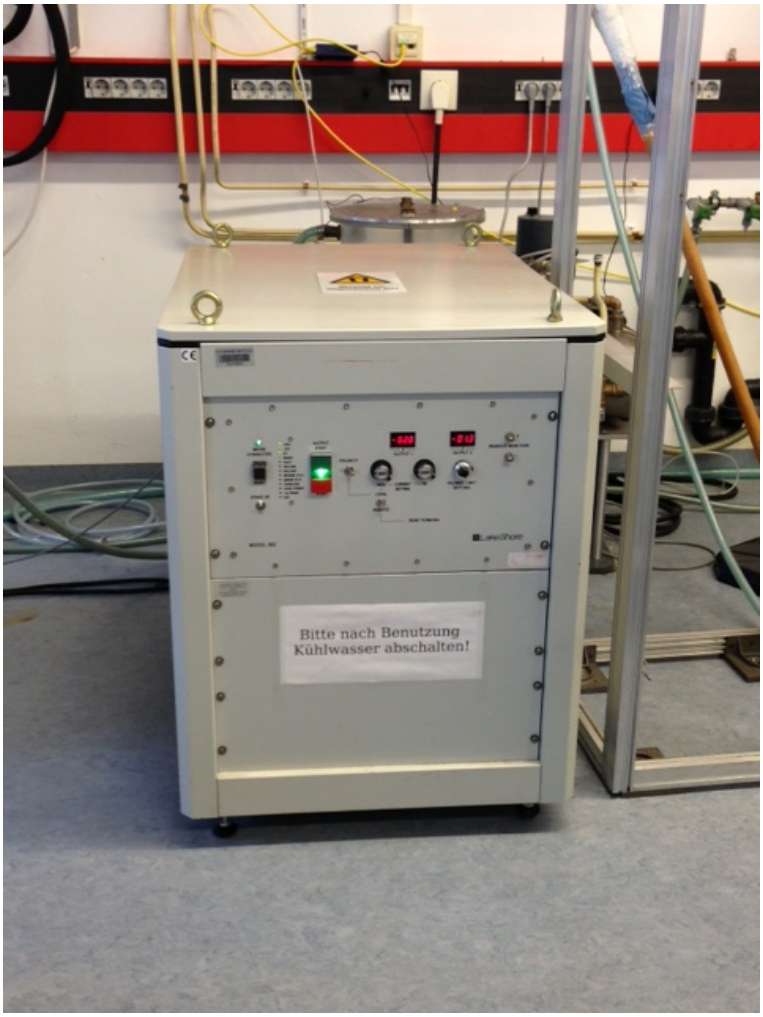

FIG. 6. Power supply

4. turn on the gauss meter field controller and set field to zero. (local, zero probe, enter)

B. measurement

1. create folder for saving data. copy the required measurement files. (4 text files) to this folder.

2. check the measurement files. (a) fieldscan values (b) VNA settings.

3. start measurement labview programme, copy the measurement folder path to the programme, and start.

4. during the measurement, check if the field follows accordingly and if VNA is responding

FIG. 7. Gauss meter

reading from the front panel.

5. after the measurement, go to the measurement folder and copy the ".....measurement" to combine file programme and run it.

6. open matlab data reading programme, change the meas folder to ".....store" and run the programme to obtain the gray scale data plot.

7. save the data to origin for calculating the group velocity of spin wave.

C. Post-measurement

1. turn off all the programmes.
2. turn off the power supply and cooling water.
3. turn off the gauss meter.
4. turn off the VNA.

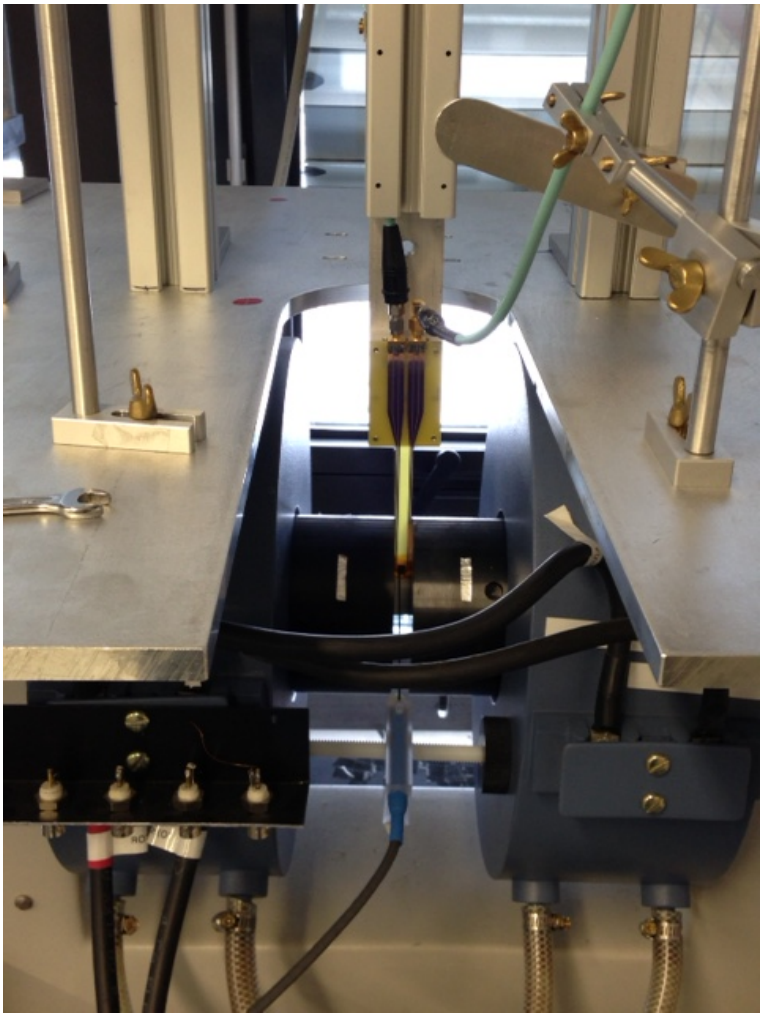

FIG. 8. magnet and sample holder

VI. REFERENCE TO READ

1. Stancil, D. D. and Prabhakar, A. Spin Waves: Theory and Applications. Appendix C (Springer 2009).

2. Dirk Grundler, Fabian Giesen, and Jan Podbielski: Spin Waves in the Inhomogeneous Internal Field of Nanostructured Rings, book article in : Spin Wave Confinement, S. Demokritov (ed.), World Scientific (2008).

3. V.V. Kruglyak, S.O. Demokritov, and D. Grundler: "Magnonics", J. Phys. D: Applied Physics 43, 264001 (2010).

4. H. Yu, R. Huber, T. Schwarze, F. Brandl, T. Rapp, P. Berberich, G. Duerr, and D. Grundler: "High propagating velocity of spin waves and temperature dependent damping

in a CoFeB thin film". Appl. Phys. Lett. 100, 262412 (2012) .